Characterizing complex fluids with high frequency rheology using torsional resonators at multiple frequencies

Gerhard Fritz

Polymer Research Division, BASF Aktiengesellschaft, D-67056 Ludwigshafen, Germany

Wolfgang Pechhold

Institut für dynamische Materialprüfung an der Universität Ulm, D-89081 Ulm, Germany

Norbert Willenbacher[a)]

Polymer Research Division, BASF Aktiengesellschaft, D-67056 Ludwigshafen, Germany

Norman J. Wagner

Center for Molecular and Engineering Thermodynamics, Department of Chemical Engineering, University of Delaware, Newark, Delaware 19716

(Received 4 January 2002; final revision received 4 November 2002)

Synopsis

A set of torsional resonators is used to characterize the linear viscoelastic behavior of complex fluids in the kilohertz range. The frequency dependence of the elastic and loss modulus of a hard sphere dispersion, electrostatically and electrosterically stabilized particles, worm-like micelles, polystyrene microgels, and polymer solutions is studied. The results are compared to theoretical predictions for these systems. The utility of the instrument for characterizing the high frequency rheology of complex fluids is demonstrated. This is especially relevant for suspensions or dilute solutions and gels, where time-temperature superposition often fails and the relaxation spectrum is inaccessible from conventional oscillatory shear rotational rheometry. © *2003 The Society of Rheology.* [DOI: 10.1122/1.1538608]

I. INTRODUCTION

The rheological properties of complex fluids at high frequencies are of great interest for the investigation of microstructure and interactions, as well as for determining dynamical properties. A classic example is the elastic modulus G'_∞ of molecular fluids, which is directly linked to the interaction potential and the equilibrium microstructure [Zwanzig and Mountain (1965)]. Extending this theory to colloidal suspensions [Buscall and co-workers (1982), Russel and co-workers (1989), Wagner (1993), Bergenholtz and

[a)]Author to whom all correspondence should be addressed; electronic mail: norbert.willenbacher@basf-ag.de

co-workers (1998)] offers a fascinating and relatively simple possibility to probe the interaction potential in concentrated colloidal samples. These theories assume the applied shear field to vary much faster than the characteristic relaxation time of the Brownian particles, i.e., $a^2\omega/D_S \gg 1$, with a as the particle radius and D_S as the self-diffusivity. However, as relatively high frequencies must be achieved in order to probe G'_∞ for typical aqueous dispersions, there are only a few published studies of the true, high frequency elasticity of liquid colloidal dispersions.

The classical theories of polymer dynamics in solution [Rouse (1953), Zimm (1956)], and in the melt [Doi and Edwards (1986)] and their extensions predict various power-law behaviors at high frequencies that contain information about the fluid's relaxation mechanisms. Hence, high frequency rheology can probe molecular architecture and solvent-polymer interactions. For example, branched polymers exhibit Rouse motion at very high frequencies, but the hierarchical relaxation of the segments can result in characteristic features in the high frequency regime that distinguish them from linear analogs [see, e.g., McLeish (1988), Blackwell and co-workers (2001), or Larson (2001)].

Combining these theoretical approaches with high frequency rheological measurement techniques may also offer new insight into the hydrodynamic properties of polymers adsorbed or grafted onto colloidal particles and the stability of these particles [Elliott and Russel (1998)].

The earlier-mentioned Zwanzig and Mountain equation and its application to colloidal fluids predicts a frequency-independent, high frequency elastic modulus, where high frequency is defined relative to the Brownian relaxation time of a particle. However, calculations for dispersions of hard-spheres with surface roughness predict a limiting power-law frequency dependence of 1/2 [Lionberger and Russel (1994)]. Theories for other complex fluids with internal structure, such as polymer solutions or worm-like micelles predict power-law behavior in the kilohertz regime with frequency exponents in the range of 1/2–3/4, before ultimately becoming frequency independent (the frequency dependence of the solvent appears in the gigahertz range). Consequently, *accurate* measurement of the frequency dependence of the elastic modulus at high frequencies can provide important insight into the dynamical properties and microstructure of complex fluids.

Conventional rheometers are usually limited to frequencies $\leqslant 100$ Hz due to mechanical limitations and inertial effects in the gap loading limit. In many cases, these frequencies are not high enough to reach the true high frequency limiting behavior. The extension of the accessible frequency range by means of superposition techniques, as described for example by Ferry (1980) (time-temperature or time-concentration superposition) is not always possible due to particles or self-assembled microstructures that are sensitive to temperature, concentration, and the physical properties of the solvent.

Torsional resonators, such as those first explored by Mason (1949), are capable of achieving higher frequencies, up to the megahertz regime. Various experimental designs have been employed [Oosterbroeck and co-workers (1980), Blom and Mellema (1984), van den Ende and co-workers (1992), Bergenholtz and co-workers (1998)], but often the measurements are limited to one frequency. Multiple frequencies are required to either prove the existence of a high frequency plateau [Horn and co-workers (2000)] or to determine the frequency exponent for comparison to theory. The set of torsional nickel resonators developed by Mellema and Blom [Oosterbroeck and co-workers (1980), Blom and Mellema (1984), van den Ende and co-workers (1992), Bergenholtz and co-workers (1998)], the lumped resonators of Schrag and Johnson (1971) that have been improved by Hvidt and co-workers (1982) [Nakken and co-workers (1994), Nakken and co-workers

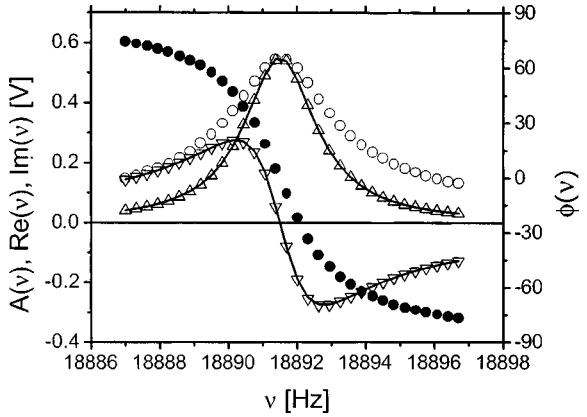

FIG. 1. Amplitude [$A(\nu)$,○] and phase [$\varphi(\nu)$,●] measured for an unloaded resonator. The real [Re(ν),△] and imaginary [Im(ν),▽] parts calculated from Eq. (1) are approximated by the theoretical resonance expressions [Eq. (2), lines].

(1995)], and the torsional rod of Stokich and co-workers (1994) are among the few examples where multiple, high frequencies are obtained in a consistent set of devices.

A newly developed set of two torsional resonators is presented here, giving access to the storage and loss modulus of low viscosity fluids at five different frequencies between 3.7 and 57 kHz. The experimental setup and calibration of the instrument is described. Several examples are presented to demonstrate the efficacy of the instrumentation for characterizing the high frequency rheology of complex fluids. Specifically, we examine the frequency dependence of the high frequency elastic modulus of the following model systems: hard spheres colloidal suspensions, electrostatically and electrosterically stabilized polymer dispersions, colloidal microgels in organic solvents, worm-like micelles and polymer solutions.

II. THEORY

Torsional resonators are excited at frequencies ν in the vicinity of the resonance frequency. The experimentally accessible parameters are the voltage amplitude $A(\nu)$ of the response and the absolute value of the phase $\varphi(\nu)$ at these frequencies. The absolute value of φ is not necessary for further evaluation. Therefore, φ is set to be 0 at the maximum of the amplitude A. The measured functions can now be transformed into the real (Re) and imaginary (Im) parts

$$\begin{aligned} \mathrm{Re}(\nu) &= A(\nu)\cdot\cos(\varphi), \\ \mathrm{Im}(\nu) &= A(\nu)\cdot\sin(\varphi), \end{aligned} \tag{1}$$

which are measured by a lock-in amplifier. These functions can be approximated by a simple model for mechanical resonators that is depicted in Fig. 1:

$$\begin{aligned} \mathrm{Re}(\nu) &= A_0\cdot f\frac{D^2\nu}{(f^2-\nu^2)^2+D^2\nu^2}, \\ \mathrm{Im}(\nu) &= A_0\cdot f\frac{D(f^2-\nu^2)}{(f^2-\nu^2)^2+D^2\nu^2}, \end{aligned} \tag{2}$$

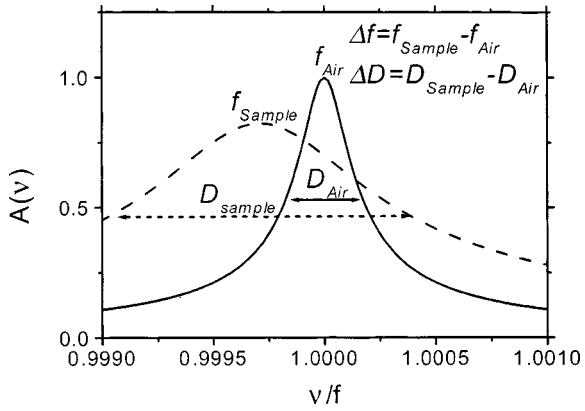

FIG. 2. Measuring principle of torsional resonators: The resonance frequency and the width of the resonance are changed relative to the values observed in air, if the resonator is immersed into the sample. The viscous and elastic properties of the sample are calculated from these two parameters.

where f is the resonance frequency, D is the damping of the oscillation, and A_0 is a constant amplitude.

The torsional motion of the resonator creates a damped shear wave in the surrounding medium. This leads to a damping of the resonator motion due to the medium's impedance. Therefore, the resonance frequency of the loaded resonator will be lower and broader than in air (Fig. 2). Pechhold (1959) has studied these phenomena with regard to different instrument configurations. For a perfect cylinder resonator of radius a and length l fully immersed into a fluid, the complex frequency shift follows from continuum mechanics [Pechhold (1959)] as

$$\Omega_m = \frac{2\Delta f_m}{f_m} + i\frac{\Delta D_m}{f_m} = \frac{4i}{m\pi}\left(1+\frac{l}{a}\right)\frac{\rho}{\rho_1}\frac{c}{c_1}, \tag{3}$$

in which $m = 1,2,3,...$ signifies the mth torsional mode (but only the odd modes can be excited by the piezoelements, embedded near the middle plane), ρ_1, c_1 density and shear wave velocity of the resonator material (titanium) and ρ, $c = \sqrt{(G' + iG'')/\rho}$ that of the viscoelastic fluid.

Solving the complex Eq. (3) via squaring it, and introducing $f_m = nc_1/2l$ (torsional eigenfrequencies with zero radial nodes), yields

$$G' = \frac{k}{\rho}\left[\left(\frac{\Delta D}{2}\right)^2 - \Delta f^2\right], \tag{4}$$

$$G'' = -\frac{l}{\rho}\Delta D\Delta f.$$

The results can be equivalently represented as viscosities through the relationships: $\eta' = G''/\omega$ and $\eta'' = G'/\omega$ using the angular frequency $\omega = 2\pi f$. In Eq. (4) earlier, $k = [\pi\rho_l la/(l+a)]^2$ is the derived instrument constant. To account for deviations from the ideal resonator behavior (e.g., due to a nonideal coupling between the metal rod and the piezoelectric crystal) we use the modified equations

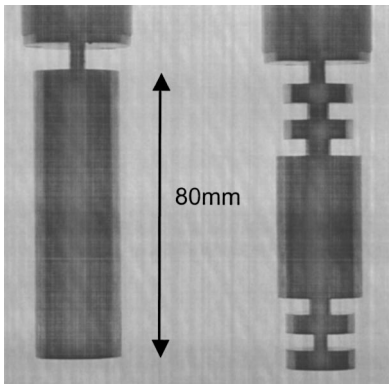

FIG. 3. Cylindrically shaped and double-dumbbell torsional resonators used. The resonators of diameter 24 mm and total length 80 mm are attached at the end of a central tube in the middle plane perpendicular to which four thickness-shear piezoelements are embedded as actor and sensor. The cylinder oscillates at 19 and 57 kHz while the dumbbell oscillates at 3.7, 19, and 38 kHz.

$$G' = \frac{k}{\rho}\cdot\left[\left(\frac{\Delta D}{2}\right)^2 - \Delta f^2\right] + \frac{k}{\rho}\cdot\frac{2c\Delta D\Delta f}{1+c^2} + d$$
$$G'' = -\frac{k}{\rho}\cdot\Delta D\Delta f + \frac{2c}{1+c^2}\cdot\frac{k}{\rho}\cdot\left[\left(\frac{\Delta D}{2}\right)^2 - \Delta f^2\right] \tag{5}$$

where two empirical constants c and d have been introduced. These have been found to be necessary to calibrate the resonators against a set of Newtonian liquids of known viscosity. Note that for an ideal resonator, the instrument constants c and d would be zero. If d is set to zero, Eq. (5) is equivalent to the relationship previously used by Bergenholtz and co-workers (1998). Here we can improve the calibration significantly by using the additional parameter d. The mixing factor c should lie in the range $0 > c \gg -1$, whereas there are no theoretical constraints on d. The values of these three coefficients are determined as a function of temperature by calibration against a set of Newtonian standards as will be described later.

III. EXPERIMENT

A. Instrument operation and temperature control

Measurements were performed with two torsional resonators (Fig. 3) constructed by the Institut für dynamische Materialprüfung, Ulm, Germany. The resonators of diameter 24 mm and total length 80 mm are attached at the end of a central tube in the middle plane perpendicular to which four thickness-shear piezoelements are embedded as actor and sensor. The resonator material is titanium. The double-dumbbell shaped resonator No. 1 is operated the frequencies 3.7, 10, and 38 kHz, while the cylindrical resonator No. 2 allows for experiments at 19 and 57 kHz. This corresponds to a range of angular frequencies $\omega\ (=2\pi\nu)$ from 23 000 up to 358 000 rad s^{-1}. Excitation of the oscillation and detection of the voltage amplitude and the phase are done with a DSP lock-in amplifier (model SR850, Stanford Research Systems).

In order to obtain G' and G'' from the resonance frequency and the damping of the loaded resonator, the corresponding values for the unloaded resonator have to be subtracted. Since these quantities strongly depend on temperature, they have been deter-

TABLE I. Resonance frequency f_0 and Damping D_0 of unloaded resonators at 0 °C and Temperature dependence corrections m_1 and m_2 for the frequency and n_1 for the damping.

Resonator	f_0	m_1	m_2	D_0	n_1
1	3720.29	−0.8480	−0.000 353	1.06	−0.007 76
1	10 077.74	−2.3300	−0.000 471	2.63	−0.010 00
1	38 206.61	−9.9800	−0.001 590	3.97	0.018 80
2	19 081.59	−5.0168	−0.000 755	8.66	−0.008 00
2	57 389.05	−14.6200	−0.008 420	12.63	−0.011 42

mined experimentally in a broad temperature range. They can be described by the following empirical equations, which are used to subtract the resonance characteristics of the unloaded resonator from the corresponding data of the loaded instrument:

$$f(T) = f_0 + m_1 T + m_2 T^2, \tag{6}$$

$$D(T) = D_0 + n_1 T,$$

where T is the temperature in degrees Celsius, m_i and n_i are instrument constants, and f_0 and D_0 are the frequency and damping of the unloaded resonator in air at a certain reference temperature, which was taken to be 0 °C in our experiments (Table I, Fig. 4).

Samples are placed into a cylindrical double-walled sample cell and the temperature is controlled by a liquid thermostat and measured by a PT-100 temperature sensor within the resonators and processed with a digital thermometer (INFT series, Newport Electronics). All experiments reported here were done at 20.0 ± 0.1 °C unless stated otherwise. Temperature stability during the individual experiments was 0.01 °C. The gap between resonator and sample cell is 1 mm. As the penetration depth of the excited wave is significantly lower than this for our samples, the instrument operates in the surface loading limit as will be discussed further.

B. Calibration and reproducibility

The resonators were calibrated by measuring a series of Newtonian fluids of known viscosity (η', while $\eta'' = 0$) at 20 °C: Milli-Q-water, Baysilone siliconoil KT 3 (KT 3, Bayer), Baysilone siliconoil M 10 (M 10, Bayer), Palatinol C (C, BASF Aktiengesellschaft), Palatinol AH (AH, BASF Aktiengesellschaft), silicon oil AP 100 (AP 100, Wacker Chemie), silicon oil PN 200 (PN 200, Bayer). The changes in frequency and damping were transformed into η'_{exp} and η''_{exp} values. (Table II)

The instrument constants *k*, *c*, and *d* were varied until the quantity Δ reaches the global minimum

$$\Delta = \sum \left(\frac{\eta'_{\text{exp}} - \eta'_{\text{known}}}{\eta'_{\text{known}}} \right)^2 + \sum \left(\frac{\eta'_{\text{exp}}}{\eta'_{\text{known}}} \right)^2. \tag{7}$$

The resulting parameters are listed in Table III. A comparison between the target viscosities of the fluids and the best approximations for the resonator results are given in Fig. 5. Obviously, a consistent calibration of the resonators is achieved in the whole viscosity range except for the 3.7 kHz resonance. This resonance frequency corresponds to an antiparallel oscillatory motion of the two outer disks of the double-dumbbell resonator. In this case the signal has to cross both bridges of the dumbbell. This causes an extra damping and, hence, a low signal-to-noise ratio. Therefore, significant deviations

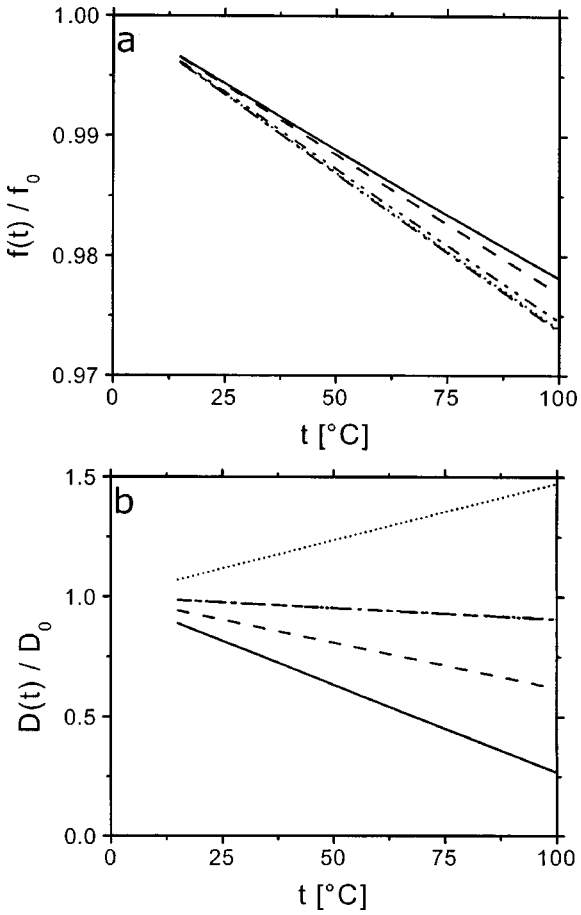

FIG. 4. Temperature dependence of the frequency (a) and damping (b) relative to the reference values (0 °C). 3.7 (solid), 10 (dashed), 38 (dotted), 19 (dash-dotted), and 57 kHz (dash-dot-dotted).

are observed at higher viscosities and raw data are rejected for samples with $|\eta^*| > 20$ mPa s. All frequencies show the strongest deviations at low viscosities. This may be attributed to the effect of some additional constant damping after sample loading (caused for example by the inertia of the sample or slightly imperfect shear).

The calibration and its application to viscoelastic samples has been validated by comparing the torsional resonator results with those obtained by time temperature superposition for a 30% polystyrene solution in ethylbenzene using a Rheometrics RFS II rheometer (Fig. 6). Absolute values as well as frequency dependence agree for G' and G''.

Tests for reproducibility show that repeated measurements of the same sample (including repetition of the measurement of the unloaded resonator) have a standard deviation of less than 8% for G' (on average 6.2%). The standard deviations of the measured G'' values are typically less than 5% (on average 3.4%).

While the range of the calibration liquids establishes limits for accessible G'', the G' range is not so well defined. However, the upper limit $G'_{\max}$ for the accessible elastic moduli can be estimated from the maximum damping measured $\Delta D_{\max}$ for the viscous calibration liquids. Since Δf should be close to 0 for a purely elastic sample, Eq. (5) can be simplified to

TABLE II. Newtonian liquids of known viscosities (η', $\eta'' = 0$) used for calibration of the resonators and the corresponding approximations. The cells with no value indicate sample-resonator combinations that could not be accurately measured.

	Water	KT 3	M 10	C	AH	AP 100	PN 200
η' (mPa s)	1.01	2.73	9.95	20.31	79.6	129.8	252.1
$\eta'_{3.7\ \mathrm{kHz}}$	1.39	3.02	9.15	17.1	⋯	⋯	⋯
$\eta''_{3.7\ \mathrm{kHz}}$	−0.24	−0.47	0.19	2.95	⋯	⋯	⋯
$\eta'_{10\ \mathrm{kHz}}$	1.24	3.11	10.24	19.2	69.8	113.2	221.9
$\eta''_{10\ \mathrm{kHz}}$	0.58	0.08	−0.67	−1.2	0.30	2.7	8.1
$\eta'_{38\ \mathrm{kHz}}$	1.11	2.88	9.83	20.9	73.4	115.4	220.7
$\eta''_{38\ \mathrm{kHz}}$	−0.13	0.02	−0.07	−0.71	−0.19	3.34	27.7
$\eta'_{19\ \mathrm{kHz}}$	1.10	3.04	10.7	20.1	76.3	123.9	253.8
$\eta''_{19\ \mathrm{kHz}}$	−0.11	−0.05	−0.03	−0.02	0.55	1.0	13.1
$\eta'_{57\ \mathrm{kHz}}$	1.17	3.59	10.5	20.6	77.0	125.6	249.4
$\eta''_{57\ \mathrm{kHz}}$	0.09	0.32	−0.01	0.08	−0.67	0.69	22.7

$$G'_{\max} = \frac{k}{\rho}\left(\frac{\Delta D_{\max}}{2}\right)^2 + d. \tag{8}$$

This expression simplifies further to $G'_{\max} = G''_{\max}/2$ for a perfect resonator according to Eq. (4). If one wants to stay within the parameter range used for calibration this corresponds to a $G'_{\max}$ of 50 kPa.

This estimation agrees well with the limits established experimentally. The resonators described here enable elastic modulus measurements in the range 50 Pa $< G' <$ 50 kPa. If G' is lower, the change of the resonance curve cannot be measured accurately enough. The upper limit is estimated from samples where the resonators and time temperature superposition gave consistent results [see later and Willenbacher and Pechhold (2000)], but might be actually higher.

C. Samples

Several colloidal and polymeric systems have been examined to determine their frequency dependent elastic modulus and viscosity with the torsional resonators.

- Charge neutralized Stöber-silica particles have been prepared and characterized by Maranzano and Wagner (2001) and Maranzano and co-workers (2000). The particles

TABLE III. Calibration constants k, c, and d for the accessible resonance frequencies f_0 and the standard excitation voltages V_0 of the resonances.

Resonator	f_0 (Hz)	V_0 (V)	k (kg^2 m^{-4})	c	d (Pa)
1	3720.29	2.0	3526.2	−0.0972	0.00
1	10 077.74	1.0	3957.5	−0.1173	109.43
1	38 206.61	0.2	14 164.5	−0.0515	0.00
2	19 081.59	0.2	19 831.7	−0.0462	0.00
2	57 389.05	0.2	20 089.0	−0.0278	−33.54

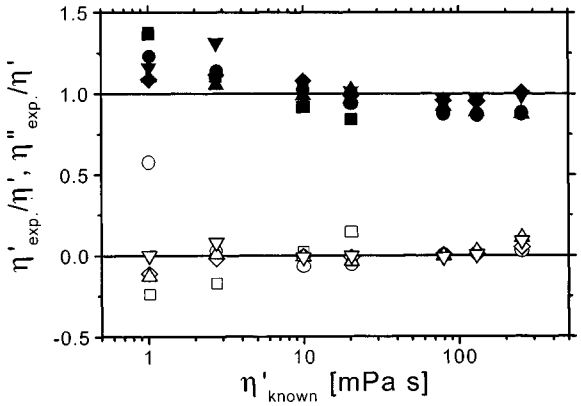

FIG. 5. Results of the Newtonian liquids used for calibration: 3.7 (■), 10 (●), 19 (♦), 38 (▲), and 57 kHz (▼). Closed symbols mark η' values, open η''. Data for calibration of the 3.7 kHz frequency have been used only up to 20 mPa s due to weak signals at higher viscosities.

have a diameter of 302 ± 26 nm [by transmission electron microscopy (TEM)]. Dispersing them in the index matching tetrahydrofurfuryl alcohol reduces van der Waals attractions, while charge neutralization minimizes electrostatic repulsion. Small angle neutron scattering and intrinsic viscosity measurements confirm the hard sphere character.

- A monodisperse poly(styrene) (PS) dispersion with a diameter of 107 nm (by TEM) and a surface charge density of 9 μC/cm^2 (by conductometric titration) [Horn and co-workers (2000)].
- Electrosterically stabilized particles consisting of a core of 54% poly(butyl acrylate) and 46% polystyrene and a stabilizing grafted layer of 5% or 8% (w/w, relative to core) poly(methacrylic acid) (PMAA) [Fritz and co-workers (2002b)]. The core diameter is 95 and 109 nm, respectively the thickness of the grafted layer strongly depends on solvent pH and ionic strength. This layer collapses at low pH, but it forms a brush like

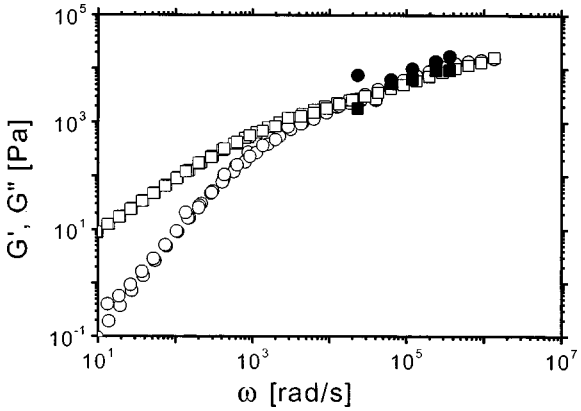

FIG. 6. Validation of G' (■) and G'' (●) measured with torsional resonators by comparing with results obtained for a 30% polystyrene solution in ethylbenzene by time-temperature superposition [G' (○) and G'' (□)]

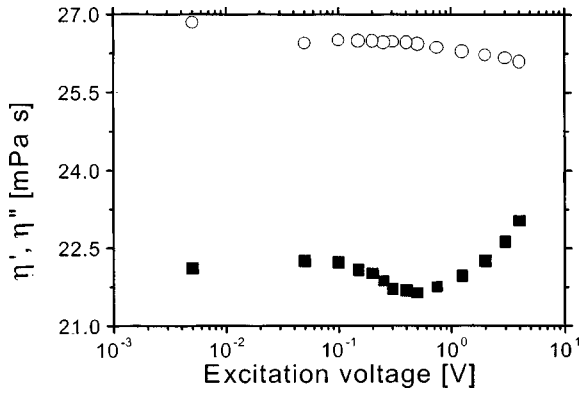

FIG. 7. Amplitude variation, given in terms of the excitation voltage, for a dispersion, stabilized with 8% PMAA, $\phi_{\text{eff}} = 0.725$, at 19 kHz. η' (■) and η'' (○).

shell at high *p*H. Therefore steric effects control stability at *p*H 7 and above while electrostatic interactions dominate at low *p*H.

- PS-microgel particles were donated by Eckert and Bartsch, Institute of Physical Chemistry, University of Mainz [Bartsch and co-workers (1998)]. These particles consist of linear poly(styrene) chains between 1,3-diisopropenylbenzene branching points and are swollen in 2-ethylnaphtaline. Two crosslink densities, 1:50 and 1:10 in terms of number ratio of linear and branching monomers, were studied. The particles are spherical with a diameter of 384 nm.
- A solution of 30 wt % polystyrene (BASF Aktiengesellschaft, commercial grade Polystyrene 148 H, $M_W = 250\,000$ g/mol) in ethylbenzene was prepared to examine the high frequency behavior of concentrated polymer solutions.
- Solutions of 100 mM cetylpyridium chloride in 250 mM sodium salicylate with 0.00, 0.63, and 1.01 g/ml sucrose were provided by Fisher, ETH Zürich, Switzerland. For further details see Fischer and Rehage (1997).

IV. RESULTS

A. Linear viscoelastic response

For our piezoelectrically driven torsional resonators the amplitude of the input voltage can be varied between 0.004 and 5 V. The linearity of the response signal has been checked for various samples. A typical result is shown in Fig. 7. The decrease of η'' and the minimum in η' as the excitation voltage increases indicate the onset of nonlinear behavior which may be caused by the sample or the resonator itself. The data presented later have been obtained at input voltages in the linear response.

The propagation of the shear wave has a strong impact on dynamic mechanical measurements [Schrag (1977), White and Schrag (1999)]. According to Mason (1949) and Thurston (1964) the shear wave propagates a characteristic distance δ in the medium

$$\delta = \sqrt{\frac{2}{\rho\,\omega^2} \cdot \frac{G'^2 + G''^2}{\sqrt{G'^2 + G''^2} - G'}}. \tag{9}$$

The penetration depth has been checked for all samples and was typically less than 100 μm and in all cases less than 350 μm. Such penetration is considerably smaller than the

gap width between the resonator and the sample container wall (1 mm). Therefore, the surface loading limit applies and the maximum deformation of the surrounding fluid can be estimated according to Mason (1949):

$$\gamma_{\max} = \Omega\,\delta^{-1} = \Omega\sqrt{\frac{\rho\,\omega^2}{2}\cdot\frac{\sqrt{G'^2+G''^2}-G'}{G'^2+G''^2}}. \tag{10}$$

The oscillation amplitude Ω at the resonator surface is not known exactly but it is estimated to be around 50 nm for a typical excitation voltage of 0.2 V. From Eq. (10) the deformation amplitude can then be estimated to be below 1% for the samples studied here.

B. Colloidal dispersions

The main objective of this study is to characterize the frequency dependence of colloidal suspensions with different stabilization in the high frequency limit where the applied shear field is much faster than the Brownian motion of the colloidal particles, i.e., $\omega/2\pi \gg D_S^S/l^2 \approx D_0/a^2$, with l as the mean interparticle separation, a as the particle radius, D_S^S as the short-time self diffusivity and D_0 as the bare diffusion coefficient [Bergenholtz and co-workers (1998), Horn and co-workers (2000)]. This criterion is clearly fulfilled for the samples investigated here at frequencies beyond 0.3 kHz. Therefore, the frequencies probed are clearly within the high frequency regime.

In all cases investigated here the frequency dependence of the moduli can be approximated by a power-law $G' \approx A_0'\omega^{n_e}$, $G'' \approx A_0''\omega^{n_\nu}$ in the frequency range accessible with our resonators. The resulting exponents are summarized in Table IV. The data are plotted versus frequency in Figs. 8 and 9. Figure 10 shows the normalized moduli of representative systems for the different classes of fluids.

According to Lionberger and Russel (1994) hard-sphere dispersions should exhibit either a high frequency plateau for the elastic modulus, or, if the no-slip boundary condition at the particle surface is not fully met, a $\omega^{1/2}$ dependence. For the hard sphere silica suspension investigated here the exponent $n_e = 0.70 \pm 0.11$ is found to describe the high frequency dependence of G'. Note, the relatively low absolute value of the elastic modulus for this system makes these measurements difficult and leads to a fairly high uncertainty in the slope. Nevertheless, our result is in reasonable agreement with the theoretical prediction mentioned earlier and with experimental data for another hard sphere silica system investigated by van der Werff and co-workers (1989). Within the framework of the Lionberger and Russel theory a surface roughness of about 2.5 nm is estimated to be responsible for the observed frequency dependence of the high frequency modulus [Fritz and co-workers (2002a)]. Also in agreement with expectation and previous measurements, the loss modulus is observed to vary linearly with frequency, which is a consequence of the dominance of the hydrodynamic contribution to the viscosity.

Colloidal dispersions with a finite-range potential, such as electrostatically stabilized systems should show a finite limiting value for the elastic modulus at high frequency, corresponding to $n_e = 0$. For the electrostatically stabilized dispersions investigated here we find a weak frequency dependence in G' ($n_e = 0.10 \pm 0.03$). This is slightly higher than the theoretical prediction. As the system contains counterions and the double layer will thus have dynamical properties, it is tempting to attribute this slight frequency dependence to double-layer relaxation phenomena. However, given the characteristic double layer thickness of $l \sim 3$ nm and an ion diffusivity in the double layer of $D_{\text{ion}} \sim 10^{-9}$ m^2/s [Russel and co-workers (1989)], even at the highest frequency,

TABLE IV. Frequency dependences $G'(\omega) = A_0'\omega^{n_e}$ and $G''(\omega) = A_0''\omega^{n_\nu}$ observed for different colloidal systems.

Sample	n_e	A_0'	n_ν	A_0''
Charged PS spheres, 0.1 mM KCl, $\phi = 41.2\%$	0.10 ± 0.03	62.08	0.84 ± 0.03	2.9×10^{-2}
5% PMAA, *p*H 4, 10 mM NaCl, 34.3% (w/w)	0.09 ± 0.06	44.18	0.80 ± 0.03	4.2×10^{-2}
5% PMAA, *p*H 5, 105 mM NaCl, 34.2% (w/w)	0.26 ± 0.06	6.64	0.86 ± 0.01	2.9×10^{-2}
5% PMAA, *p*H 7, 100 mM NaCl, 33.8% (w/w)	0.22 ± 0.02	305.62	0.70 ± 0.03	0.78
5% PMAA, *p*H 9, 260 mM NaCl, 32.3% (w/w)	0.25 ± 0.04	94.32	0.86 ± 0.03	7.8×10^{-2}
8% PMAA, *p*H 7, 100 mM NaCl, 29.5% (w/w)	0.34 ± 0.02	67.77	0.74 ± 0.03	0.53
Hard spheres, $\phi = 0.5$	0.70 ± 0.11	0.13	1.05 ± 0.04	3.4×10^{-2}
30% PS in ethylbenzene	0.53 ± 0.05	16.50	0.53 ± 0.06	8.9
Cetylpyridium micelles in water	0.46 ± 0.14	0.63	0.78 ± 0.04	3.9 ± 10^{-2}
Cetylpyridium in 0.63 g/ml sucrose solution	0.62 ± 0.05	0.44	1.11 ± 0.06	2.9×10^{-3}
Cetylpyridium in 1.01 g/ml sucrose solution	0.61 ± 0.07	1.02	1.15 ± 0.09	4.4×10^{-3}
PS microgels, 1:10 crosslinked, $\phi_{\text{eff}} = 0.604$	1.00 ± 0.09	5.8×10^{-3}	1.02 ± 0.04	2.9×10^{-2}
PS microgels, 1:50 crosslinked, $\phi_{\text{eff}} = 0.612$	1.10 ± 0.14	1.4×10^{-3}	0.91 ± 0.04	$5.8\times10_{-2}$

$\omega l^2/D_{\text{ion}} < 10^{-3}$ and the double layer can be considered to be relaxed on the time scale of this measurement. Further, hydrodynamic interactions may also be considered as static even at the highest frequency as $\omega a^2\rho/\mu < 10^{-4}$, where ρ and μ refer to the solvent density and viscosity. In conclusion, the weak frequency dependence observed here at low elasticities probably indicates the limit of experimental accuracy for our resonators

The rheology of the PMAA-grafted electrosterically stabilized system strongly depends on *p*H and ionic strength of the solvent, this is discussed in detail elsewhere [Fritz and co-workers (2002b)]. At *p*H 4, the stabilizing brushes are collapsed and electrostatic interactions dominate. Correspondingly, the high frequency modulus is almost independent of frequency ($n_e = 0.09\pm0.06$), and similar to that of the charge stabilized dispersion. At *p*H 5, however, the PMAA layer starts to swell and a stronger frequency dependence is observed ($n_e = 0.26\pm0.06$). A further increase in *p*H does not change the frequency dependence of G' significantly, $n_e = 0.22\pm0.02$ and $n_e = 0.25\pm0.04$ are found for *p*H = 7 and *p*H = 9, respectively. Increasing the amount of grafted PMAA from 5% to 8% leads to an even stronger frequency dependence of G' (e.g., $n_e = 0.34\pm0.02$ for *p*H 7, 100 mM NaCl, Fig. 8).

Obviously, the presence of the swollen polyelectrolyte brush induces the observed frequency dependence in G'. Assuming that the relaxation of the polyelectrolyte chains in the brush simply superimposes to the frequency independent relaxation of the particles it is qualitatively clear that this contribution increases with frequency. The brush relaxation time can be calculated according to Wittmer and co-workers (1994) as $\tau_1 \cong \mu L^3/k_BT$, with the solvent viscosity μ, the Boltzmann constant k_B, and the absolute temperature T. Typical brush lengths are about 20 nm yield $0.04 < \omega\tau_1 < 0.71$, which suggests that there may be a contribution from the elasticity of the polymer in the

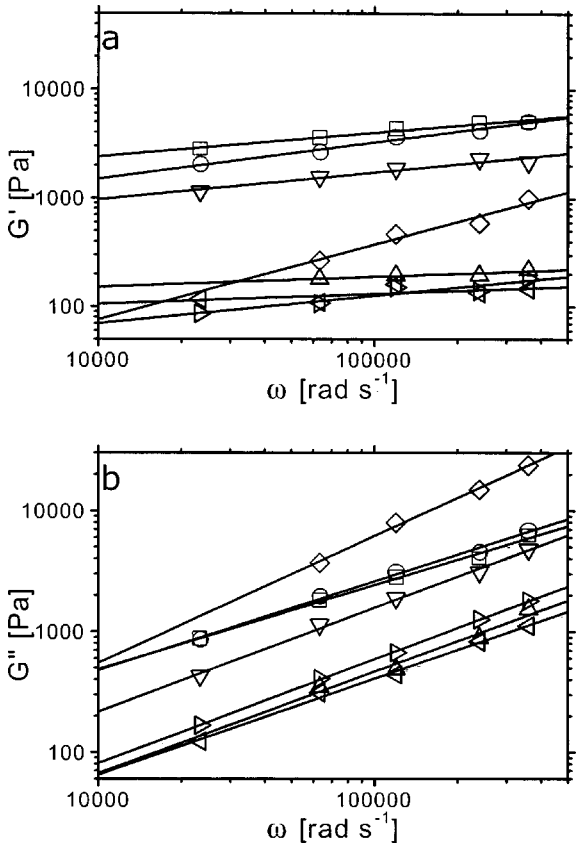

FIG. 8. High frequency elastic and loss moduli of disperse systems: hard spheres ($\phi = 0.5$) (◇), electrostatically stabilized PS particles in 0.1 mM KCl (△), sterically stabilized particles with 5% PMAA layer (pH 4, 34.3%, 10 mM NaCl, (◁), pH 5, 34.2%, 105 mM NaCl (▷), pH 7, 33.8%, 100 mM NaCl (□), and pH 9, 32.3%, 260 mM NaCl (▽)) and sterically stabilized particles with 8% PMAA layer at pH 7, 100 mM NaCl, 29.5% (○).

brush. Therefore, the observed increase in frequency dependence of the elastic modulus with increasing electrosteric brush length is a possible manifestation of relaxation processes within the polyelectrolyte brush on the times scale of the experiment.

In summary, the frequency dependence of G' in the kilohertz range may be used as a fingerprint for a concentrated colloidal suspension, which immediately tells whether it is stabilized electrostatically, sterically or whether it resembles hard sphere behavior. Interestingly, the loss modulus for the electrosteric and electrostatic stabilized dispersions is observed to grow with frequency sublinearly. This is probably a consequence of the loss modulus being comparable to the elastic modulus in strength over this frequency range; hence, the loss modulus has contributions from relaxation modes in the microstructure as well as the purely dissipative contributions from hydrodynamic interactions.

C. Polymer solutions and cross-linked polymers

Turning now to particles with internal structure, PS-microgels would be expected to show a complex relaxation behavior in this frequency regime. Almost linear frequency dependence is observed over the accessible range. The exponent $n_e = 1.00 \pm 0.09$ for a

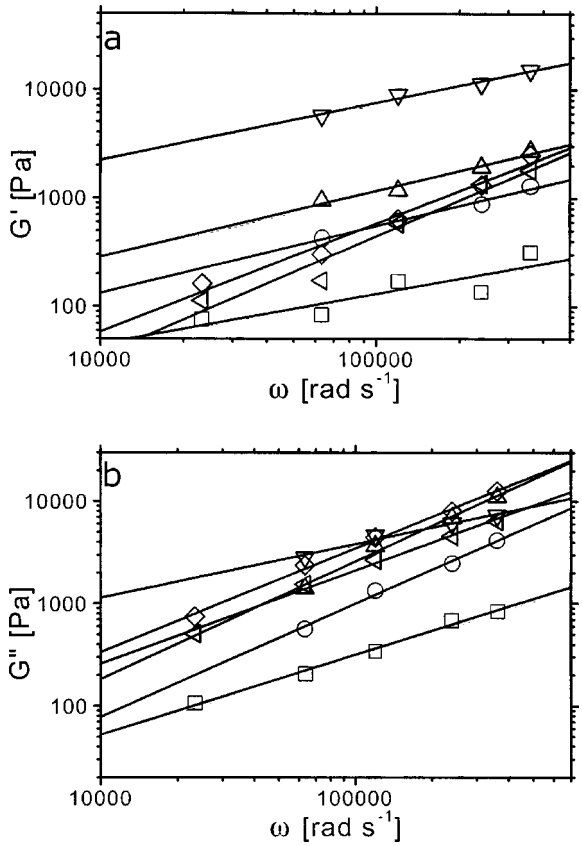

FIG. 9. High frequency elastic and loss moduli of worm like cetylpyridium cloride micelles in sodium salicylate solutions with sucrose. 0 g/ml sucrose (□), 0.63 g/ml (○), 1.01 g/ml (△), of a 30% PS solution (▽) and of microgels cross-linked 1:10 (◇) and 1:50 (◁).

1:10 cross-linked gel at $\phi_{\text{eff}} = 0.604$ and $n_e = 1.10 \pm 0.14$ for a 1:50 cross-linked gel at $\phi_{\text{eff}} = 0.612$ (Table IV). The distinct frequency dependence found reflects internal relaxation modes of the microgel particles. For reference, the loss modulus is significantly greater than the elastic modulus, and is observed to vary nearly linearly with frequency as well. We are unaware of any corresponding theoretical prediction for comparison.

For the concentrated PS solution in ethylbenzene $n_e = 0.53 \pm 0.05$ and $n_\nu = 0.53 \pm 0.06$ over the frequency range studied here. This frequency dependence has been confirmed independently using time-temperature superposition and data from conventional rotational rheometry [Willenbacher and Pechhold (2000), Fig. 6], which yields $n_e = 0.49 \pm 0.01$ in the corresponding frequency range. This is in good agreement with $n_e = n_\nu = 0.5$ as predicted by the classical Rouse theory [Rouse (1953)] for this frequency range.

Sufficiently long worm-like micelles are experimentally analogous to solutions of semi-flexible polymers in good solvent. According to Morse (1998) such systems change from the behavior predicted by a Rouse–Zimm model with slopes between $n_e = 1/2$ and $n_e = 2/3$ [Rouse (1953), Zimm (1956)] to $n_e = 3/4$ scaling that is characteristic for the worm-like character if they are loosely entangled. Experimentally, the systems in sucrose solution yield an average value of 0.62 (see Table IV, Fig. 9). Sucrose

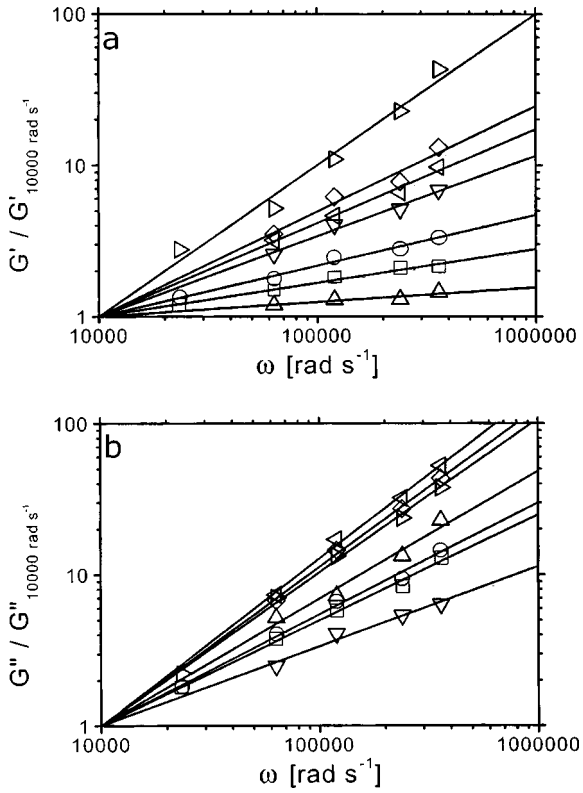

FIG. 10. High frequency elastic and loss moduli scaled by the extrapolated value at 10 000 rad s^{-1}. Hard spheres ($\phi = 0.5$) (◇), sterically stabilized particles with 5% PMAA layer (pH 7, 100 mM NaCl (□) and sterically stabilized particles with 8% PMAA layer (pH 7, 100 mM NaCl) (○), electrostatically stabilized PS particles in 0.1 mM KCl (△), cetylpyridium micelles in 0.63 g/ml sucrose solution (◁), polystyrene microgels, crosslinked 1:10 (▷), and a 30% polystyrene solution in ethylbenzene (▽|).

is added to increase the background viscosity, which also reduces the characteristic relaxation time. In water without sucrose, the measured frequency dependence decreases to a value of $n_e = 0.46 \pm 0.14$, and the absolute value of G' (75 Pa) at the lowest resonator frequency is also quite close to the 50 Pa observed with a Couette system by Fischer and Rehage (1997). This change in slope with sucrose addition may signal that the measurements in water are not in the high frequency limit. Our measurements for high sucrose levels are in quantitative agreement with the range of the Rouse–Zimm model, but do not show an added contribution from weak entanglements as predicted by Morse. The addition of sucrose raises the purely dissipative contributions to G'' sufficiently such that the loss modulus is observed to increase linearly with frequency over the range studied.

V. CONCLUSIONS

The results demonstrate that the frequency dependence of the elastic shear modulus can be used to distinguish microstructures in complex fluids, and as such, provides a powerful and robust method for investigating complex, multiphase, and microstructured fluids. The viscoelastic properties of polymer solutions measured with a series of high frequency resonators agree with results obtained from classical rheometry and time-temperature superposition, validating the experimental apparatus. It is demonstrated that

these resonators can provide results for samples where superposition techniques fail, due to temperature sensitivity or solvent restrictions. These resonators are also of interest for probing fragile structures such as suspensions in the linear viscoelastic range. Well-known theoretical predictions for the frequency dependence of G' for very different complex fluids, i.e., dispersions of electrostatically stabilized spheres and concentrated polymer solutions, are confirmed, which validates the experimental setup. The technique also gives new insight into the relaxation behavior of more complicated systems like microgels, worm-like surfactant solutions, and electrosterically stabilized dispersions, providing information that is relevant from an academic as well as applied industrial point of view (i.e., stability).

ACKNOWLEDGMENTS

The authors want to thank P. Fischer (ETH Zürich) for the cetylpyridium chlorid solutions, V. Schädler (BASF Aktiengesellschaft) for the electrosterically stabilized particles, W. Richtering (Christian-Albrechts-Universität Kiel) for providing us with the electrostatically stabilized particles, and E. Bartsch and Th. Eckert (Johannes-Gutenberg-Universität Mainz) for the microgels.

References

Bartsch, E., S. Kirsch, P. Lindner, T. Scherer, and S. Stolken, ''Spherical microgel colloids—hard spheres from soft matter,'' Ber. Bunsenges. Phys. Chem. **102**, 1597–1602 (1998).

Bergenholtz, J., N. Willenbacher, N. J. Wagner, B. Morrison, D. van den Ende, and J. Mellema, ''Colloidal charge determination in concentrated liquid dispersion using torsional resonator oscillation,'' J. Colloid Interface Sci. **202**, 430–440 (1998).

Blackwell, R. J., O. G. Harlen, and T. C. B. McLeish, ''Theoretical linear and nonlinear rheology of symmetric treelike polymer melts,'' Macromolecules **34**, 2579–2595 (2001).

Blom, C., and J. Mellema, ''Torsion pendula with electromagnetic drive and detection system for measuring the complex shear modulus of liquids in the frequency range 80–2500 Hz,'' Rheol. Acta **23**, 98–105 (1984).

Buscall, R., J. W. Goodwin, M. W. Hawkins, and R. H. Ottewill, ''Viscoelastic properties of concentrated lattices. 2. Theoretical-analysis,'' J. Chem. Soc., Faraday Trans. 1 **78**, 2889–2899 (1982).

Doi, M., and S. F. Edwards, *The Theory of Polymer Dynamics*, (Clarendon, Oxford, 1986).

Elliott, S. L., and W. B. Russel, ''High frequency shear modulus of polymerically stabilized colloids,'' J. Rheol. **42**, 361–378 (1998).

Ferry, J. D., *Viscoelastic Properties of Polymers*, 3rd ed. (Wiley, New York, 1980).

Fischer, P., and H. Rehage, ''Rheological master curves of viscoelastic surfactant solutions by varying the solvent viscosity and temperature,'' Langmuir **13**, 7012–7020 (1997).

Fritz, G., B. J. Maranzano, N. J. Wagner, and N. Willenbacher, ''High frequency rheology of hard sphere colloidal dispersions measured with a torsional resonator,'' J. Non-Newtonian Fluid Mech. **102**, 149–156 (2002a).

Fritz, G., V. Schädler, N. J. Wagner, and N. Willenbacher, ''Electrosteric stabilization of colloidal dispersions,'' Langmuir **18**, 6381–6390 (2002b).

Horn, F. M., W. Richtering, J. Bergenholtz, N. Willenbacher, and N. J. Wagner, ''Hydrodynamic and colloidal interactions in concentrated charge-stabilized polymer dispersions,'' J. Colloid Interface **225**, 166–178 (2000).

Hvidt, S., F. H. M. Nestler, M. L. Greaser, and J. D. Ferry, ''Flexibility of myosin rod determined from dilute solution viscoelastic measurements,'' Biochem. J. **21**, 4064–4073 (1982).

Larson, R. G., ''Combinatorial rheology of branched polymer melts,'' Macromolecules **34**, 4556–4571 (2001).

Lionberger, R. A., and W. B. Russel, ''High frequency modulus of hard-sphere colloids,'' J. Rheol. **38**, 1885–1908 (1994).

Maranzano, B. J., N. J. Wagner, G. Fritz, and O. Glatter, ''Surface charge of 3-(trimethoxysilyl) propyl methacrylate (TPM) coated Stöber silica colloids by zeta-phase analysis light scattering and small angle neutron scattering,'' Langmuir **16**, 10556–10558 (2000).

Maranzano, B. J., and N. J. Wagner, ''The effects of particle size on reversible shear thickening of concentrated colloidal dispersions,'' J. Chem. Phys. **114**, 10514–10527 (2001).

Mason, W. P., ''Measurement of the viscosity and shear elasticity of liquids by means of a torsionally vibrating crystal,'' Trans. ASME **69**, 359–370 (1949).

McLeish, T. C. B., ''Hierarchical relaxation in tube models of branched polymers,'' Europhys. Lett. **6**, 511–516 (1988).

Morse, D. C., ''Viscoelasticity of concentrated isotropic solutions of semiflexible polymers. 2. Linear response,'' Macromolecules **31**, 7044–7067 (1998).

Nakken, T., G. H. Nyland, K. D. Knudsen, A. Mikkelsen, and A. Elgsaeter, ''A new torsional rod instrument for high frequency dynamic viscoelastic measurements,'' J. Non-Newtonian Fluid Mech. **52**, 217–232 (1994).

Nakken, T., K. D. Knudsen, A. Mikkelsen, and A. Elgsaeter, ''Dynamics of coaxial torsional resonators consisting or segments with different radii, material properties and surrounding media,'' Rheol. Acta **34**, 235–247 (1995).

Oosterbroeck, M., H. A. Waterman, S. S. Wisall, E. G. Altena, J. Mellema, and G. A. M. Kip, ''Automatic apparatus, based upon a nickel-tube resonator, for measuring the complex shear modulus of liquids in the kHz range,'' Rheol. Acta **19**, 497–506 (1980).

Pechhold, W., ''Eine methode zur messung des komplexen schubmoduls im frequenzbereich 1–100 kHz,'' Acustica **9**, 39–48 (1959).

Rouse, P. E. J., ''A theory of the linear viscoelastic properties of dilute solutions of coiling polymers,'' J. Chem. Phys. **21**, 1272–1280 (1953).

Russel, W. N., D. A. Saville, and W. R. Schowalter, *Colloidal Dispersions* (Cambridge University Press, New York, 1989).

Schrag, J. L., and R. M. Johnson, ''Application of the Birnboim multiple lumped resonator principle to viscoelastic measurements of dilute macromolecular solutions,'' Rev. Sci. Instrum. **42**, 224–232 (1971).

Schrag, J. L., ''Deviation of velocity gradient profiles from the 'gap loading' and 'surface loading' limits in dynamic simple shear experiments,'' Trans. Soc. Rheol. **21**, 399–413 (1977).

Stokich, T. M., R. R. Radtke, C. C. White, and J. L. Schrag, ''An instrument for precise measurement of viscoelastic properties of low viscosity dilute macromolecular solutions at frequencies from 20 to 500 kHz,'' J. Rheol. **38**, 1195–1210 (1994).

Thurston, R. N., ''Wave propagation in fluids and normal solids,'' in *Physical Acoustics: Principles and Methods*, Vol. 1, Part A, edited by W. P. Mason (Academic, New York, 1964), pp. 1–110.

Wagner, N. J., ''The high-frequency shear modulus of colloidal suspensions and the effects of hydrodynamic interactions,'' J. Colloid Interface Sci. **161**, 169–181 (1993).

van den Ende, D., J. Mellema, and C. Blom, ''Driven torsion pendulum for measuring the complex shear modulus in a steady shear flow,'' Rheol. Acta **31**, 194–205 (1992).

van der Werff, J. C., C. G. de Kruif, C. Blom, and J. Mellema, ''Linear viscoelastic behavior of dense hard-sphere dispersions,'' Phys. Rev. A **39**, 795–807 (1989).

White, C. C., and J. L. Schrag, ''Theoretical predictions for the mechanical response of a model quartz crystam microbalance to two viscoelastic media: A thin sample layer and surrounding bath medium,'' J. Chem. Phys. **111**, 11192–11206 (1999).

Willenbacher, N., and W. Pechhold, ''Torsional resonance oscillation—New prospects for an old technique,'' Proceedings of the XIIIth International Congress on Rheology, Cambridge, UK, 2000, Vol. 3, pp. 69–71.

Wittmer, J., A. Johner, and J. F. Joanny, ''Some dynamic properties of grafted polymer layers,'' Colloids Surf., A **86**, 85–89 (1994).

Zimm, B. H., ''Dynamics of polymer molecules in dilute solutions: Viscoelasticity, flow birefringence and dielectric loss,'' J. Chem. Phys. **24**, 269–278 (1956).

Zwanzig, R., and R. D. Mountain, ''High frequency elastic moduli of simple fluids,'' J. Chem. Phys. **43**, 4464 (1965).